BBA - Biomembranes 1862 (2020) 183125

Contents lists available at ScienceDirect

BBA - Biomembranes

journal homepage: www.elsevier.com/locate/bbamem

Factors influencing the solubilization of membrane proteins from *Escherichia coli* membranes by styrene–maleic acid copolymers☆

Adrian H. Kopf*,[1], Jonas M. Dörr[1], Martijn C. Koorengevel, Federico Antoniciello, Helene Jahn, J. Antoinette Killian*

Membrane Biochemistry & Biophysics, Bijvoet Center for Biomolecular Research and Institute of Biomembranes, Utrecht University, Padualaan 8, 3584CH Utrecht, the Netherlands

ARTICLE INFO

Keywords:
Styrene-maleic acid (SMA)
Native nanodisc
KcsA
Solubilization efficiency
Environmental factors
pH-dependence

ABSTRACT

Styrene–maleic acid (SMA) copolymers are a promising alternative to detergents for the solubilization of membrane proteins. Here we employ *Escherichia coli* membranes containing KcsA as a model protein to investigate the influence of different environmental conditions on SMA solubilization efficiency. We show that SMA concentration, temperature, incubation time, ionic strength, presence of divalent cations and pH all influence the amount of protein that is extracted by SMA. The observed effects are consistent with observations from lipid-only model membrane systems, with the exception of the effect of pH. Increasing pH from 7 to 9 was found to result in an increase of the solubilization yield of *E. coli* membranes, whereas in lipid-only model systems it decreased over the same pH range, based on optical density (OD) measurements. Similar opposite pH-dependent effects were observed in OD experiments comparing solubilization of native yeast membranes and yeast lipid-only membranes. We propose a model in which pH-dependent electrostatic interactions affect binding of the polymers to extramembraneous parts of membrane proteins, which in turn affects the availability of polymer for membrane solubilization. This model is supported by the observations that a similar pH-dependence as for SMA is observed for the anionic detergent SDS, but not for the nonionic detergent DDM and that the pH-dependence can be largely overcome by increasing the SMA concentration. The results are useful as guidelines to derive optimal conditions for solubilization of biological membranes by SMA.

1. Introduction

In the past years, styrene–maleic acid (SMA) copolymers have been used to isolate a wide range of membrane proteins differing in size and properties in the form of native nanodiscs (e.g. [1–7]). These nanodiscs provide a stable environment for membrane proteins, which facilitates their isolation and purification. In addition, the nanodiscs offer a convenient platform for structural and functional characterization of the entrapped protein (e.g. [8–14]). For some of these downstream applications it may be a challenge to obtain a sufficiently high yield of purified nanodiscs. To a large extent this yield will be determined by the efficiency with which the copolymers are able to solubilize the target membrane.

Much information on factors that determine the efficiency of solubilization has been obtained from studies on model membrane systems [15–17]. It was found that solubilization generally increases with increasing SMA concentration and temperature, and that also the presence of salt promotes solubilization. However, the presence of divalent cations impedes solubilization by inducing aggregation [18–20] and a similar effect was found for a low pH [21–23]. In addition, it was shown that the nature of the target membrane plays a key role in determining the efficiency of solubilization, with solubilization for example being less efficient for lipids when they are in a liquid-ordered or in a gel phase or when the lipids contain negatively charged head groups [15,16,24].

A particular intriguing parameter for solubilization is the pH value.

Abbreviations: SMA, styrene-maleic acid; OD, optical density; *E. coli*, *Escherichia coli*; DMPC, 1,2-dimyristoyl-*sn*-glycero-3-phosphocholine; DOPC, 1,2-dioleoyl-*sn*-glycero-3-phosphocholine; PLE, polar lipid extract; DDM, *n*-Dodecyl-beta-D-Maltopyranoside; SDS, sodium dodecyl sulfate; MLV, multilamellar vesicles; OMP, outer membrane protein

☆ This article is part of a Special Issue entitled: Native Membranes

* Corresponding authors.
E-mail addresses: a.h.kopf@uu.nl (A.H. Kopf), j.a.killian@uu.nl (J.A. Killian).

[1] Equal contributions.

https://doi.org/10.1016/j.bbamem.2019.183125
Received 3 September 2019; Received in revised form 17 October 2019; Accepted 10 November 2019
Available online 15 November 2019

SMA has two acid groups per maleic acid unit, which have different pKa values (pK_1 ~5.5, pK_2 ~8.6, [21]). As a result SMA polymers have an optimal pH range in which they are active. At lower pH increasing protonation of the maleic acid groups leads to aggregation, while at higher pH the increasing charge density of the polymers makes them more hydrophilic and may affect their conformational behavior, ultimately resulting in a decreased solubilization efficiency [21]. The optimal pH range was tested in phosphatidylcholine (PC) vesicles for SMA copolymers with different average styrene-to-maleic acid ratios and it was found that SMA copolymers with a ~2:1 ratio of styrene-to-maleic acid are most efficient for solubilization over a large pH range and provide the highest stability for the nanodiscs [25].

While model membrane studies have yielded many insights into the role of different parameters on solubilization efficiency of SMA, systematic studies on biological membranes are still scarce. Available reports so far focused mainly on comparison of the solubilization efficiency of commercially available polymer variants that differ in composition and average length [26–28]. Here it was found that polymers with an average styrene-to-maleic acid ratio of ~2:1 and a relatively short length are most efficient in solubilizing native membranes, followed by polymers with a ~3:1 styrene-to-maleic acid ratio [27–29]. This is very similar to results obtained in model membrane studies with respect to both composition [21,30] and length [31].

In order to rationalize membrane protein solubilization by SMA from biological membranes we here use a SMA copolymer with an average styrene-to-maleic acid ratio of ~2:1 and a relatively short length (M_n ~2.5 kDa) [27–29] to systematically investigate the influence of various environmental parameters on the solubilization efficiency of *Escherichia coli* membranes overexpressing the tetrameric channel protein KcsA as a model protein.

KcsA was chosen as a model protein because of several reasons: (i) it can be obtained in membranes at high copy numbers due to its spontaneous membrane insertion and oligomerization, constituting one of the most abundant proteins after initiated gene expression [3,32,33], (ii) the robustness of the protein allows studies at a wide range of conditions with small impact on structural integrity of the protein, and (iii) the stability of the KcsA tetramer during sodium dodecylsulfate polyacrylamide gel-electrophoresis (SDS–PAGE) [32,34] allows for a simple means of identification of the target protein band.

The KcsA solubilization experiments were complemented with turbidimetric measurements to compare the kinetics of SMA solubilization in *E. coli* with those in other membrane systems, including model membranes of synthetic lipids. The results help to identify relevant parameters for membrane solubilization and to determine optimal experimental conditions for solubilization of membrane proteins by SMA or other copolymers.

2. Materials & methods

2.1. Materials

All phospholipids were purchased from Avanti Polar Lipids (Alabaster, AL). The lipids used were: 1,2-dimyristoyl-*sn*-glycero-3-phosphocholine (DMPC), 1,2-dioleoyl-*sn*-glycero-3-phosphocholine (DOPC), *E. coli* polar lipid extract, and yeast (*S. cerevisiae*) polar lipid extract. *n*-Dodecyl-beta-D-Maltopyranoside (DDM) was obtained from Anatrace (Maumee, OH). The styrene–maleic anhydride copolymer, Xiran 30010 (number-average molecular weight (M_n) of ~2.5 kDa, weight-average molecular weight (M_w) of ~6.5 kDa, with corresponding polydispersity index (PDI) of ~2.6, and a styrene-to-maleic anhydride ratio of ~2), was a kind gift from Polyscope Polymers (Geleen, NL). Sodium dodecyl sulfate (SDS) and all other chemicals were obtained from Sigma Aldrich (St. Louis, MO).

2.2. Preparation of SMA solutions

Conversion of the polymers into the acid form was achieved by hydrolysis under base-catalyzed conditions as described earlier [35]. Lyophilization was generally omitted since it was not found to have a significant effect on sample quality. SMA stock solutions were prepared at final concentrations of 1% or 5% (*w/v*) in Tris base solution at 10 mM (pH unadjusted) per 1% (*w/v*) of SMA. The desired pH of the solution was adjusted by adding NaOH.

2.3. Preparation of E. coli membranes

Total membrane fractions of *E. coli* cells producing KcsA were obtained as described previously [4]. Briefly, cells were transformed with the plasmid containing the His-tagged KcsA gene and were grown with or without IPTG induction of gene expression until cultures reached an OD_{600} of ~0.8. Cells were then harvested by centrifugation and stored as pellets at −80 °C. Membrane preparations were obtained by differential centrifugation after cell wall lysis and mechanical disruption through French press [3]. To remove any remaining soluble proteins, the obtained membrane pellet was resuspended in buffer (5 mM Tris-HCl, pH 8, 150 mM NaCl, 10 mM KCl) and sedimented again by ultracentrifugation at 100,000 ×*g*.

Membrane pellets corresponding to 800 mL of cell culture were resuspended in 2–4 mL buffer (5 mM Tris-HCl in order to be able to readily adjust the pH, 300 mM NaCl, 15 mM KCl, pH 8) to an OD_{600} of ~4. After lipid extraction according to a modified version of the method of Bligh and Dyer [36], the total phosphate content was determined to be 10 mM using the method of Rouser et al. [37]. Membrane suspensions were aliquoted and stored at −20 °C until further use.

2.4. Solubilization of KcsA from E. coli membranes

Membrane pellets were thawed on ice and diluted into solubilization buffer (50 mM Tris-HCl at the desired pH, 300 mM NaCl, 15 mM KCl) to a final volume of 100 µL, with the membrane material corresponding to a final phosphate content of 1.5 mM, and a total protein concentration of approximately 1 mg/mL of which ~25% is KcsA (determined using BCA protein assay kit and densitometry of SDS-PAGE with BSA as standard, respectively). Standard solubilization was performed in buffer of 50 mM Tris-HCl, pH 8.0, 300 mM NaCl and 15 mM KCl and different final concentrations of SMA or other solubilizing agent. For standard experiments, samples were incubated for 2 h in an Eppendorf sample mixer that was set to shaking at 600 rpm at a temperature of 25 °C. Variations were made in one parameter at a time, while keeping other conditions constant.

After incubation at the desired conditions, the suspensions were subjected to centrifugation at 21,000 ×*g* for 60 min at 4 °C to pellet the non-soluble material. The pellet was then resuspended in 100 µL solubilization buffer containing 1% SDS. Since the presence of SMA was found to influence densitometric analysis, buffers for resuspending pellets of SMA-containing samples were supplemented with the corresponding amount of polymer. Both supernatant and pellet samples were then mixed with 4× concentrated SDS–PAGE (non-reducing) Laemmli sample buffer and aliquots were loaded on 13% acrylamide gels. After ~1 h of electrophoresis at 175 V, gels were fixed and stained in a 0.1% (*w/v*) solution of Coomassie Blue R-250 in water:methanol:acetic acid (70:20:10 by volume) for 1 h. Destaining was achieved by gentle agitation overnight in a solution of water:methanol:acetic acid (70:20:10 by volume).

For the evaluation of the effect of different parameters on solubilization efficiency the standard solubilization conditions were adjusted in the following ways: (i) In experiments with different incubation times, an optimal comparison was ensured by using relatively large sample volumes of 300 µL, of which aliquots were centrifuged after different periods of incubation, (ii) experiments to assess salt concentration

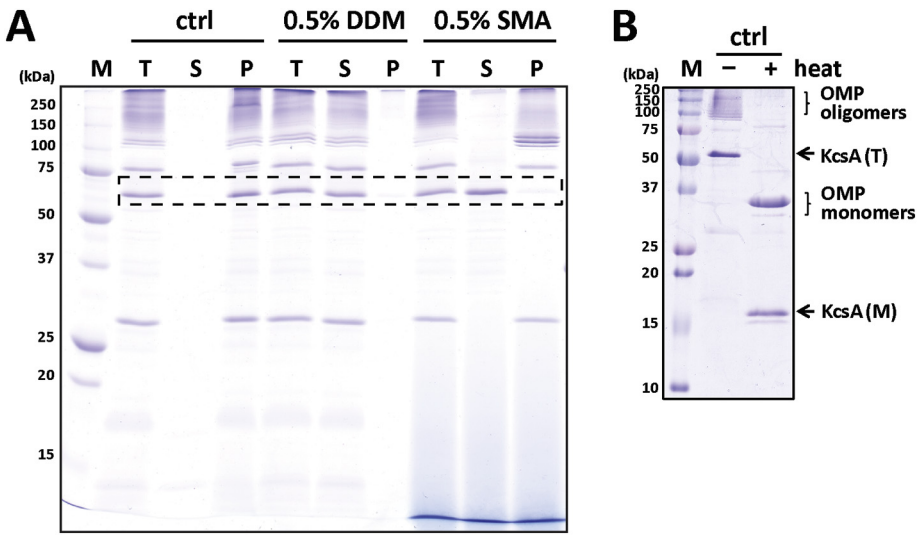

Fig. 1. (**A**) Representative coomassie-stained acrylamide gel showing solubilization of *E. coli* membranes by 0.5% (*w/v*) of DDM and SMA under standard conditions of 2 h incubation at 25 °C at pH 8 in 10 mM Tris buffer, containing 300 mM NaCl and 15 mM KCl. Total (T) samples are shown next to the supernatant (S) after ultracentrifugation and the pellet (P) that was resuspended in SDS-containing buffer. The KcsA tetramer band is highlighted by a dashed box. (**B**) Control experiment showing the conversion of the KcsA tetramer band (T) into a monomer band (M) as well as the conversion of oligomeric complexes of outer membrane proteins (OMPs) into monomers upon heating for 15 min at 95 °C in the presence of SDS.

dependence, a constant ratio of NaCl and KCl of 20:1 was used to ensure protein stability. The sample devoid of NaCl contained a final concentration of 5 mM KCl, (iii) for experiments at different pH values, SMA stock solutions at 1% (*w/v*) in 10 mM Tris were prepared at every pH value used. In addition, 100 mM Tris stock solutions were prepared at the same pH values. Samples were then mixed in a ratio that yielded a final Tris concentration of 20 mM at the desired pH. Control experiments were performed with 0.25% (*w/v*) DDM instead of SMA at otherwise identical conditions.

2.5. Densitometric analysis

Destained gels were scanned using an Epson Perfection V850 Pro scanner (Long Beach, CA) at 600 dots per inch (dpi) for general validation. The area of the gel containing KcsA bands was additionally scanned at 1200 dpi for densitometry. The band intensity was determined using the Quantity One software package (Biorad, Hercules, CA) using the volume contour tool. Values were corrected for background intensity that was determined by analyzing an area of approximately 4 times that of the band in its immediate surroundings.

For densitometric analysis of the solubilization efficiency of KcsA, we compared the intensity of the tetramer band in the solubilized fraction relative to the sum of the intensities of the solubilized and non-solubilized fractions. This procedure was chosen because, for reasons that are not understood, a straightforward comparison of the KcsA bands from the solubilized and initial samples before centrifugation often resulted in apparent solubilization yields far above 100% (up to 150%) for SMA-containing samples. For all data shown, KcsA bands from every independent sample were analyzed in duplicate pairs of solubilized and non-solubilized fractions, with each pair being loaded on a different gel.

2.6. Preparation of lipid model membranes

Lipids were dried from a chloroform stock solution under a stream of N_2 in a heated (~40 °C) bath and further dried in a desiccator under high vacuum for at least 1 h. Multilamellar vesicles were obtained by hydrating the lipid films in H_2O containing 150 mM NaCl at a concentration of 20 mM, the hydration process was performed at 37 °C for at least 30 min, with occasional swirling, followed by 7 freeze-thaw cycles. The concentrated lipid stocks were diluted to 0.5 mM in buffer consisting of 50 mM Tris-HCl (at desired pH, 7–9), 300 mM NaCl, 15 mM KCl, and then subjected to a further 3 freeze-thaw cycles.

2.7. Turbidimetry experiments

Turbidimetry experiments were conducted as described previously [15] on biological as well as lipid-only membranes. SMA polymers and samples were diluted separately in buffer (50 mM Tris-HCl Buffer, 300 mM NaCl, 15 mM KCl) with the desired pH and temperature. For the lipid-only vesicles a 0.5 mM phospholipid concentration was used, and a final SMA concentration 0.1% (*w/v*). For the biological membranes the concentration of phospholipid used was estimated to be 0.5 mM, based on total phosphate basis [37], and a final SMA concentration of 0.25% (*w/v*) was utilized. All experiments were also performed at a SMA concentration of 1% (*w/v*). Changes in the absorbance at 350 nm were detected using a UV–Vis spectrometer Lambda 18 from Perkin Elmer. After each experiment the pH of the samples was measured and the change in pH was not > 0.2 units at most.

2.8. Isolation of yeast mitochondria

For turbidimetry experiments mitochondria were isolated from yeast strain D273-10B as described [38]. Briefly, yeast cells were grown in semisynthetic lactate media to an OD of ~2. After zymolyase treatment and mechanical disruption mitochondria were isolated by differential centrifugation. Mitochondrial pellets were then resuspended in 10 mM Tris-HCl, 300 mM NaCl, pH 8.2 and the phosphate content was determined after the protocol of Rouser et al. [37].

3. Results

3.1. SMA efficiently solubilizes KcsA

To determine the amount of KcsA that can be solubilized from *E. coli* inner membranes under a given set of conditions, we employed densitometric analysis of the tetramer band (~67 KDa, [33]) after separation via SDS–PAGE. Representative results are shown in Fig. 1A for the addition of 0.5% (*w/v*) of either SMA or DDM, a commonly-used head-and-tail detergent to *E. coli* membranes. Quantification of the bands showed that in both cases > 90% of the total amount of KcsA tetramer is solubilized upon incubation for 2 h at 25 °C. In case of DDM, all *E. coli* membrane proteins are solubilized efficiently. By contrast, some abundant proteins seem to be resistant against solubilization by SMA, including a band at ~30 kDa of unknown origin and a broad band pattern in the molecular weight range above 100 kDa. These latter bands are assigned to oligomers of outer membrane proteins (OMPs), based on their abundance and their conversion into an intense (monomeric) band at ~37 kDa upon heating in the presence of SDS

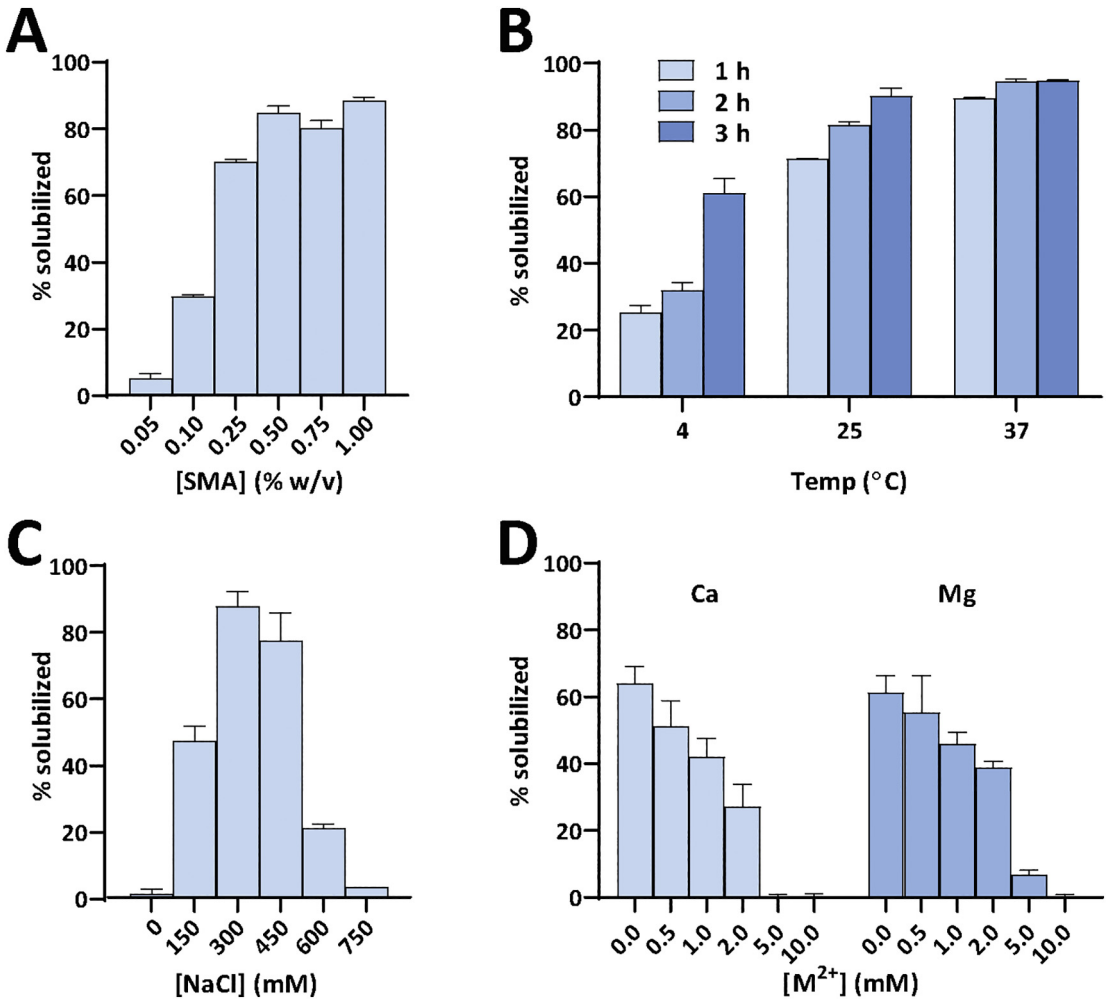

Fig. 2. Influence of various environmental parameters on solubilization of KcsA in 10 mM Tris buffer at pH 8. Other parameters were varied as indicated in the figure, with standard conditions being: 0.25% (*w/v*) SMA, 2 h incubation at 25 °C in 300 mM NaCl, 15 mM KCl. (**A**) Influence of SMA concentration. The amount of membrane material was kept constant and SMA was added at different final concentrations in the range of 0.05–1% (*w/v*). (**B**) Influence of incubation time and temperature. (**C**) Influence of salt concentration. Different amounts of NaCl were added at a constant ratio of NaCl/KCl of 20. The sample devoid of NaCl contained 5 mM KCl to ensure the structural stability of the KcsA tetramer. (**D**) Influence of divalent cations (M^{2+}). $CaCl_2$ or $MgCl_2$ was used at a concentration of 0–10 mM, all samples contained 15 mM KCl in Tris-HCl 50 mM, pH 8. Data are averages of 2 independent samples, with the error margin indicating the difference in solubilization between both samples.

(Fig. 1B).

Importantly, the results show that SMA efficiently solubilizes KcsA, which resides in the inner membrane. Fig. 1B shows that heating converts the KcsA tetramer into monomers (~18 kDa, [33]), serving as an additional tool for identification of the KcsA band. Next, we set out to determine optimal parameters for efficient KcsA extraction by SMA by systematically varying a set of environmental conditions.

3.2. Effects of SMA concentration, incubation time, temperature and ionic strength on efficiency of KcsA solubilization

In a first set of experiments the SMA concentration was varied. Fig. 2A shows that increasing the SMA concentration increases yield and efficiency of KcsA solubilization up to a maximal solubilization capacity at a SMA concentration of 0.5% (*w/v*). For variations of other experimental conditions, a SMA concentration of 0.25% (*w/v*) was chosen, since this is sufficient for significant solubilization and allows a convenient window to detect deviations in solubilization yield in both directions.

As shown in Fig. 2B, the solubilization yield of KcsA increases with increasing temperature. Prolonging the solubilization time has a favorable effect, in particular at 4 °C, where longer incubation times improve the solubilization yield by > 2-fold. At incubation temperatures of 25 °C and 37 °C solubilization conditions are quite favorable already and prolonging incubation times does not lead to a drastic improvement.

The presence of salt strongly influences solubilization yield (Fig. 2C). Hardly any solubilization is detected in the absence of NaCl, when only 5 mM KCl is present to ensure KcsA stability. Addition of increasing amounts of NaCl results in higher solubilization yields with a broad optimum range between 300 and 450 mM, where SMA solubilization is most efficient. Concentrations of NaCl exceeding this range, however, lead again to a decrease in solubilization yield.

SMA solubilization is hampered by the presence of divalent cations (Fig. 3D). All tested concentrations of divalent cations, even down to 0.5 mM, are detrimental to protein yield. In both cases there is a concentration dependency. SMA is however more sensitive to calcium as compared to magnesium, with a complete loss of solubilization at 5 mM and 10 mM, respectively. The trend and magnitude of this effect is comparable with previous studies [18–20,27].

3.3. Effects of pH on efficiency of KcsA solubilization

A major determinant of SMA properties is pH [21,39], and hence

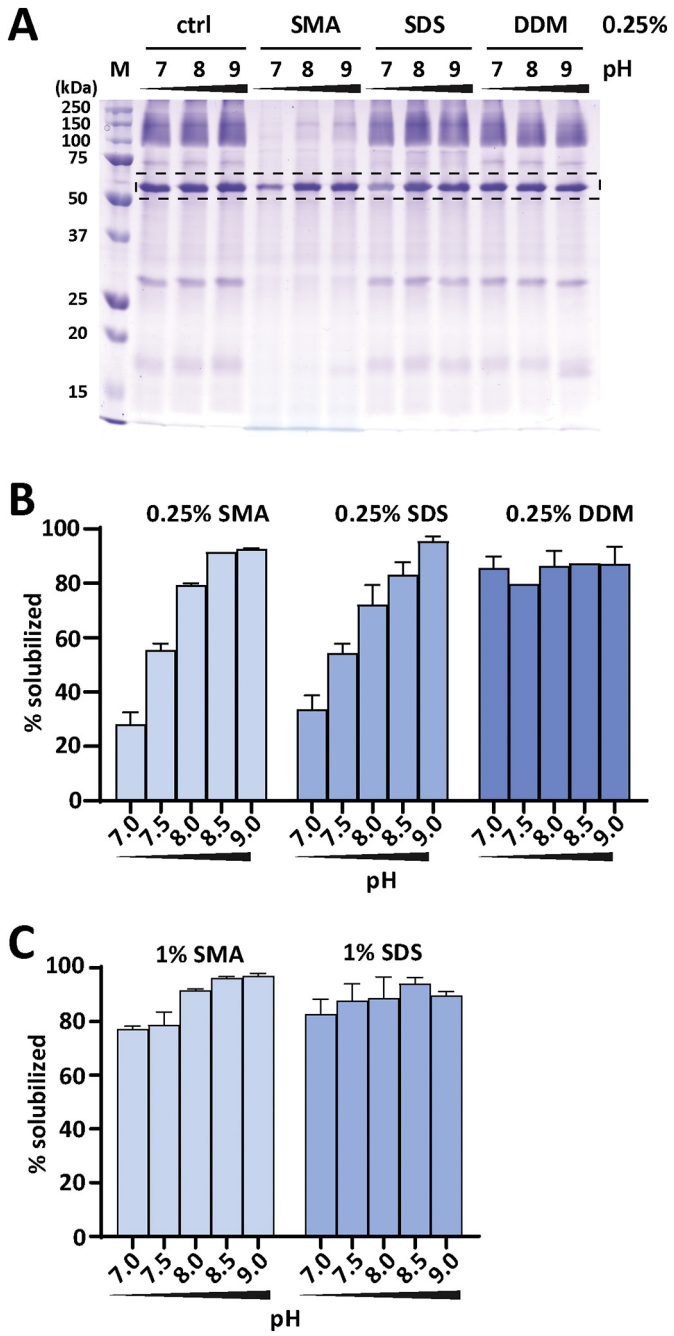

Fig. 3. pH effect on the solubilization of KcsA by SMA. (**A**) Representative SDS-PAGE showing solubilization of KcsA (highlighted by dashed box) for the total sample (ctrl) and the resulting supernatants after the addition of SMA, SDS or DDM at different pH values (pH 7–9), using a concentration of solubilizing agent of 0.25% (*w/v*). Quantification of solubilization for samples containing either (**B**) 0.25% (*w/v*) or (**C**) 1% (*w/v*) solubilizing agent, 50 mM Tris-HCl, adjusted to the desired pH, 300 mM NaCl and 15 mM KCl. All concentrations expressed are as % *w/v*. Error bars indicate the difference in solubilization between two independent experiments, data points are given as average value.

this parameter in particular might strongly influence the solubilization efficiency of KcsA. Effects of pH were monitored in the range of pH 7–9, close to physiological pH and are shown as representative gels in Fig. 3A. Further quantification shows that for SMA the solubilization yield at pH 7 is relatively low but increases dramatically at higher pH, with maximum solubilization efficiency being reached around pH 8 or 8.5. A similar pH-dependency appears to occur for other proteins on SDS-PAGE (Fig. 3A, e.g. 17, 30, and 150 kDa), suggesting that it is not a KcsA-specific effect.

To check whether the pH-dependence for SMA may be related to the charge of the polymer, we tested the effect of the non-ionic detergent DDM and the anionic detergent SDS. Solubilization by DDM shows a very different pH-dependence, with no appreciable changes in the solubilization of KcsA in the same pH range, while in case of SDS a similar pH-dependence for KcsA solubilization is observed as for SMA (Fig. 3B). These results suggest that the effects indeed are charge related.

Similar pH-dependent results were obtained at a lower concentration of SMA or when the NaCl concentration was reduced (Fig. S1A, B), further supporting the generality of the effect. However, at high SMA concentration the pH-dependence is much less pronounced and the same holds for SDS (Fig. 3C). Thus, the lower yield of solubilization of KcsA by SMA or SDS at neutral pH can be overcome by adding higher concentrations of the solubilizing agents.

The pH value used for solubilization did not appear to affect the size of the formed nanodiscs, as indicated by dynamic light scattering (Fig. S2), which showed average nanodisc sizes of hydrodynamic diameter varying in the range of 12–14 ± 2.5 nm.

The increase in SMA solubilization efficiency with increasing pH is in striking contrast with the situation in PC bilayers where solubilization as followed by turbidimetry was found to become slower with increasing pH [21]. There, the effect was attributed to the charge density on single polymer chains that leads to a higher overall hydrophilicity that impairs membrane binding and insertion [21]. However, the two systems cannot be directly compared, because the KcsA solubilization experiments performed here employ relatively long incubation times and hence this can be considered mostly an equilibrium effect, while vesicle solubilization kinetics in model membranes typically is followed on a short timescale [21] and hence the results may mostly represent a kinetic effect [30].

To gain a better understanding of the observed pH dependencies, we directly compared the solubilization kinetics in different systems by performing turbidimetry experiments on model membranes and biological membranes. In line with previous results [21], solubilization of PC model membranes was less efficient upon increasing pH. This was observed both for saturated DMPC lipids in the gel phase (Fig. 4A) as for unsaturated DOPC lipids in the fluid phase (Fig. 4B), indicating that the observed pH effect is not related to lipid packing. Importantly, also model membranes of *E. coli* polar lipids did not show an increased efficiency of solubilization at higher pH (Fig. 4C). However, when the same experiment was performed with vesicles of native *E. coli* membranes overexpressing KcsA (Fig. 4D), a reverse pH-dependence was found, in line with that observed for KcsA solubilization based on densitometric analysis (Fig. 3B). Control experiments on the solubilization of native membranes from *E. coli* not overexpressing KcsA showed a similar pH-dependency (Fig. S4).

Turbidimetry experiments were also performed at higher SMA concentrations (1% *w* > */v*). As before with gel-based assays the pH-dependency was greatly diminished. However, also at these elevated polymer concentrations the reverse pH effects between model and native membranes were still detectable (Fig. S5).

Opposite pH-dependent effects were also observed for vesicles made of the lipid extract of yeast and native yeast mitochondrial membranes (Fig. 4E, F), which have a very different protein and lipid composition [40,41]. Together, these results indicate that there is a fundamental difference between SMA solubilization of model membranes and biological membranes. The reason for these differences is most likely related to the high protein content in biological membranes, as will be further discussed below.

4. Discussion

The results in this study indicate that the efficiency of SMA solubilization of *E. coli* membranes is highly susceptible towards changes in environmental conditions. Here we will first discuss the importance of

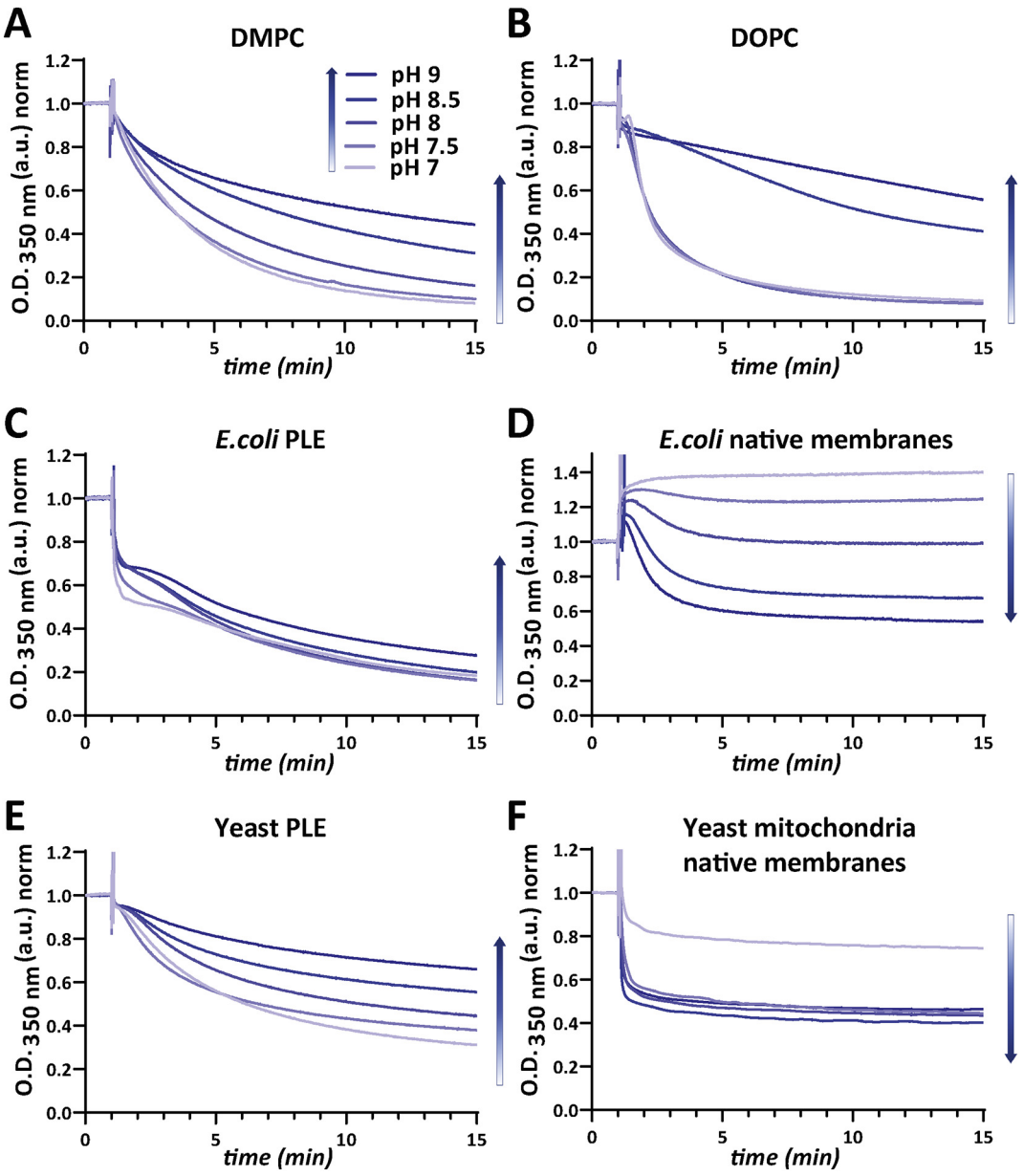

Fig. 4. pH effect on the solubilization of different membranes by SMA as observed by turbidimetry. Optical density traces at different pH values are shown for multilamellar vesicles made from DMPC (**A**), DOPC (**B**), *E. coli* polar lipid extract (**C**), or yeast polar lipid extract (**E**), as well as for *E. coli*-derived intact membrane vesicles containing KcsA (**D**), and native membranes from isolated mitochondria from yeast cells (**F**). Data are shown as normalized optical density at 350 nm ($OD_{350\ nm}$). SMA is added to the suspensions at 1 min, resulting in the high frequency noise. Data are shown as averages of two experiments. All experiments were done at a phosphate (lipid) concentration of 0.5 mM. Model membranes were tested at a final SMA concentration of 0.1% (*w/v*), and biological membranes were subjected to a SMA concentration of 0.25% (*w/v*). DMPC (**A**) and DOPC (**B**) vesicles were solubilized at 15 °C and all other experiments were performed at 25 °C.

the different parameters that were varied and then zoom in on the pH-dependent effects. Finally we will present a schematic model to explain the observed pH-dependent effects for native membranes as compared to synthetic membranes.

4.1. Role of SMA concentration

A straightforward finding of our studies is that increasing SMA concentration increases yield and efficiency of KcsA solubilization, which is line with observations in model membrane studies [15,42]. Importantly, for SMA it was found that already at concentrations of around 0.25% (*w/v*) efficient solubilization can be achieved, indicating that the high concentrations of around 2.5–3% (*w/v*) SMA that are typically used for membrane protein extraction [3,18,43,44] may be excessive. It therefore may prove useful to reevaluate these concentrations in order to avoid negative effects of free polymer on purification or other downstream processes.

It should be noted that at concentrations where KcsA was solubilized efficiently, SMA was unable to solubilize OMPs. A likely reason for this is that the *E. coli* outer membrane is highly asymmetric, with its outer leaflet containing high amounts of negatively charged lipopolysaccharide (LPS) and a network of branched sugars, that shields the membrane surface [18]. In addition, OMP porins are abundant proteins in *E. coli* [45] and a high (local) protein content may impair SMA solubilization in similar ways as in photosynthetic membranes [28,46].

The high protein content is probably also the reason why native membranes typically require more SMA for solubilization as compared to lipid-only model systems, as also shown in this study. It should be

noted however, that it is not only the concentration of SMA that is important, but also the ratio of SMA-to-lipid, or SMA-to-protein. For this reason it may be useful to experimentally determine the optimum amount of SMA per particular application.

4.2. Role of solubilization temperature and incubation time

At higher temperature a more efficient solubilization of KcsA was observed by SMA. Partly this will be simply due to the increase in thermal energy. However, changes in membrane fluidity are likely to play a larger role. Lipid extracts of the bacterial inner membrane generally show a very broad gel-to-liquid crystalline phase transition, with midpoints between 20 and 30 °C for *E. coli* cells grown at 37 °C [47,48]. At 25 and 37 °C, the membrane thus is expected to be rather fluid, facilitating efficient solubilization, and making long incubation times unnecessary. Thus, it may be worthwhile to adjust the conditions in order to optimally balance favorable solubilization kinetics to potentially unfavorable consequences such as protein degradation, when the sample is exposed to higher temperature or longer incubation times.

4.3. Role of ionic strength and divalent cations

Moderate salt concentrations in the range of 300–450 mM NaCl were found to lead to most efficient solubilization of KcsA by SMA, with both lower and higher salt concentrations causing a decrease in solubilization yields. We propose that this may be a result of different processes. Most importantly, the ionic strength may affect polymer conformation. Due to charge repulsion between the maleic acid groups, a low ionic strength could promote a long-stretched shape of the polymer that is incapable of membrane solubilization. The presence of salt ions might then make this conformation energetically less favorable, thus making SMA competent for membrane interaction and solubilization. A high ionic strength, however, may lead to the adoption of a collapsed globular conformation of SMA, since the exposure of its hydrophobic styrene units becomes more unfavorable in an increasingly polar environment. The high ionic strength might then prevent efficient solubilization by acting as a "barrier" for unburying the styrene units, which is essential for membrane binding and insertion. A preferred adoption of a collapsed conformation would be in line with the observation that at high salt concentration SMA molecules tend to aggregate and precipitate over a larger pH range (at pH < 7) than at low salt concentration [21].

Other factors that are likely to contribute to the effects of ionic strength on SMA solubilization efficiency are electrostatic interactions between SMA and negatively charged membrane lipids and between SMA and charged amino acids in the aqueous parts of membrane proteins. At low ionic strength, any repulsive or attractive electrostatic forces will be relatively strong, while increasing the ionic strength of the solution will result in screening of electrostatic interactions, thereby reducing both electrostatic repulsion and attraction and hence likely affecting solubilization [15]. Typically, these contributions to the effects of ionic strength will vary with the properties of the target membrane.

In addition to NaCl, also the presence of divalent cations can lead to aggregation and hamper solubilization. These cations will coordinate with the carboxylates of the maleic acid units, thus efficiently neutralizing their charge and thereby strongly increasing the effective hydrophobicity of SMA [7,19,27]. This may become a problem when using SMA to study membrane proteins that require divalent cations for function. Although studies have found that low millimolar concentrations of such cations may actually improve solubilization for the related but more hydrophilic copolymer, DIBMA [19], all tested concentrations used here had a negative effect on protein extraction by SMA. The absolute resistance of SMA to divalent cations is likely dependent on the presence and strength of (monovalent) salt as well as polymer composition, concentration, and pH. Thus, in cases where such divalent cations are required, further optimization of environmental conditions may be beneficial. Alternatively one could explore new developments that have been reported in the design and synthesis of related copolymers, specifically aimed to circumvent these effects, e.g. neutral polymers or polymers with positive charges [20,23,49–51]. Furthermore, several of these polymers have the additional benefit of being tolerant to a wider pH range compared to conventional SMA. However, their application for the solubilization of complex biological membranes still remains to be explored.

4.4. pH-dependence: native membranes versus model membranes

Our most remarkable finding with *E. coli* membranes is the increase in solubilization efficiency with increasing pH in the range from pH 7 to 9, which is in striking contrast with the findings for model membranes where solubilization kinetics slow down with increasing pH [21]. The latter was also observed for model membranes consisting of the polar lipid extract from *E. coli* membranes, suggesting that it is not related to lipid properties, but to the presence of proteins in the native membrane. This is supported by the observation that the same opposite trend occurs in yeast native membranes as compared to a polar extract of yeast lipids.

Interestingly, this effect was observed both by quantification of solubilization of KcsA by gel electrophoresis and by simple turbidimetry measurements on membrane fractions. This indicates that also in biological membranes turbidimetry can be a useful tool to monitor solubilization efficiency of different polymers or the effects of different solubilization conditions.

In model membranes, the pH-dependent effect was attributed to the higher charge density on single polymer chains at high pH, leading to a higher overall hydrophilicity and a long-stretched conformation that impairs membrane insertion. As the pH decreases, polymer molecules become more hydrophobic, making them more prone to interact with and insert into membranes, and hence increasing their solubilization efficiency. Upon further lowering the pH (at pH < 7), the increased hydrophobicity at some point will lead to precipitation of SMA. The pH of this aggregation point will be strongly dependent on polymer composition and on salt concentration [21].

However, polymer aggregation is likely not the cause for the lower solubilization yield at lower pH for *E. coli* membranes under the experimental conditions used here. If it were the case, decreasing the salt concentration should help since it decreases the pH of aggregation of SMA. However, a reduction of the ionic strength did not alleviate the negative effect of decreasing pH but led to a further decrease in solubilization yield (Fig. S1B). Altogether one can conclude that a different effect is at play in *E. coli* membranes which involves electrostatic interactions and is dominated by properties of the targeted membrane, but not by properties of the lipids. The results in this study suggest that this is a general effect when comparing solubilization of native membranes and lipid-only membranes. The most likely explanation for the reverse pH effect in native membranes therefore is that it is due to the presence of membrane proteins.

4.5. Role of membrane proteins

One factor that varies with pH will be the net charge on the extramembraneous parts of membrane proteins. For individual integral membrane proteins pI values have been reported from ~4.5 to 10 [52]. The *E. coli* proteome has a similar range, showing a bimodal distribution with peaks around 5.5 and 9 [53–55]. Thus in general the membrane as a whole will have an overall charge, as contributed to by all proteins in a membrane will gradually shift from positive (through net neutral) to negative upon increasing pH. We propose that this is the reason underlying the pH-dependent effects for SMA solubilization in intact membranes as observed here, according to the simplified model in Fig. 5.

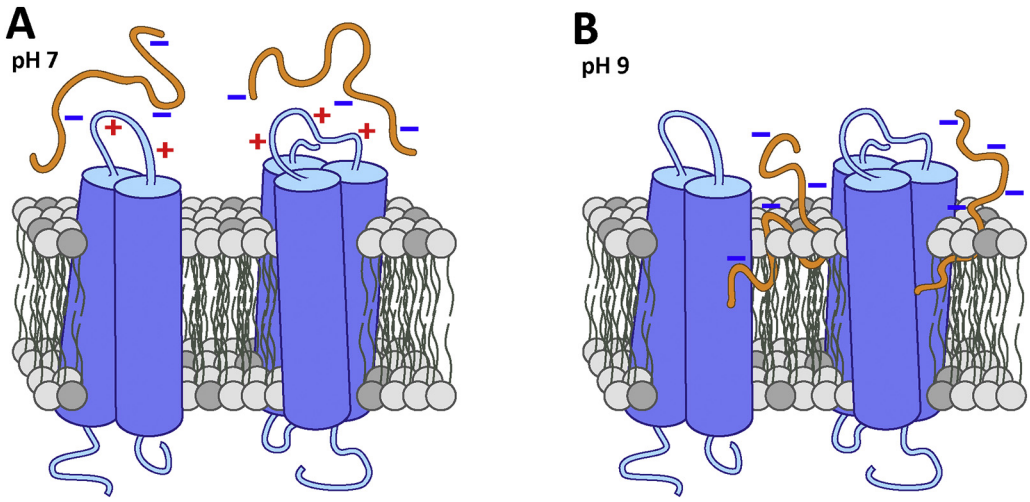

Fig. 5. Schematic drawing of proposed electrostatic model. The simplified model illustrates the interaction of negatively charged SMA copolymer with native membranes at low pH and at high pH. (**A**) At pH 7, the membrane proteins will have an overall positive charge. The negatively charged SMA molecules will tend to bind to these oppositely charged extramembraneous regions. These bound polymers will be unavailable for lipid insertion, and furthermore may hinder the binding of other polymer molecules. (**B**) At pH 9 the net charge of the membrane proteins will have shifted to be less positive to net neutral or even slightly negative, making them unattractive for SMA binding. This allows the polymers with their hydrophobic styrene moieties to bind to and insert into the lipidic core of the membrane, allowing for initiation of the solubilization process and ultimately the formation of native nanodiscs.

According to this model, upon addition of SMA to the membrane the polymer will initially encounter extramembraneous protein domains where it will tend to bind to positive charges which will be abundant at low pH. Bound SMA molecules will not be able to participate efficiently in the solubilization process, and hence less SMA will be available for solubilization. Moreover, bound SMA will decorate the membrane with an overall negative surface charge and thus may even repel binding of other polymer molecules. Upon increasing the pH, more and more proteins will become overall neutral or negatively charged and thereby become unattractive for SMA binding. Instead, at these higher pH values SMA will then preferably sample the lipid surface of the membrane and insert with its hydrophobic styrenes to initiate the solubilization process.

At high pH the polymer itself will be more charged, and thus its solubilized form becomes more favorable [21]. While this is the dominant feature to explain model membrane solubilization as a function of pH, the effect appears to be small for biological membranes where electrostatic interactions between polymer and protein seem to be more dominant. In addition, polymer concentration plays a crucial role. In general biological membranes require more polymer to be effectively solubilized compared to model vesicles (e.g. 0.25% *w/v* versus 0.1% *w/v*, respectively, at a phosphate concentration of 0.5 mM as in the present study). At these concentrations the pH is a critical factor for both systems. However, the effect is greatly diminished at elevated amounts of polymer (i.e., 1% *w/v*).

The model in Fig. 5 is supported by the observation that SMA behaves similar as SDS, but not DDM, both with respect to pH-dependence as with respect to concentration dependence. DDM is a neutral detergent and has no pH-dependency. For the anionic detergent, SDS, the pH-dependent effects are dominant when it is present at a low concentration of 0.25% *w/v* (8.67 mM). This concentration is only slightly above the CMC of SDS of 0.236% *w/v* (8.2 mM) [56,57]. Importantly, SDS is still able to completely solubilize lipid-only vesicles at this concentration, irrespective of pH (Fig. S6). Binding of SDS to proteins at lower pH can thus be expected to reduce the amount of detergent available for membrane solubilization and thereby affect the solubilization efficiency, while using a higher SDS concentration (1% *w/v*) should relieve this pH-dependency. A similar mechanism with electrostatically bound molecules being unavailable for solubilization and thereby requiring higher concentrations may hold for SMA. Thus, in considering optimal conditions for solubilization one can overcome negative effects of using high concentrations by performing experiments at higher pH and employing a lower polymer concentration, or vice versa, overcome negative effects of using lower pH by increasing the polymer concentration.

5. Conclusion and outlook

In summary, we show that many parameters affect the solubilization efficiency of SMA and that the majority of parameters derived from model membrane studies are transferable to the extraction of membrane proteins from bacterial membranes. However, pH shows a very different effect on solubilization yield and using a physiological pH of 7.4 for SMA solubilization may thus be far from the optimal to achieve efficient protein extraction. Based on the data underlying this study, a tentative recommendation for the conditions for solubilization of proteins from *E. coli* membranes can be made. This includes a moderate ionic strength (NaCl concentrations in the range of 200–500 mM), avoiding divalent cations if possible, a slightly basic pH between 8 and 9 and short incubations below 2 h at room temperature. To take into account differences in bacterial strains and culture conditions, initially trial experiments could be performed with variation of parameters that are likely to be most relevant for the particular study, such as e.g. SMA concentration or pH. The same holds for other biological membranes, where differences in membrane lipid and protein composition may change the optimal parameters for solubilization.

Supplementary data to this article can be found online at https://doi.org/10.1016/j.bbamem.2019.183125.

Transparency document

The Transparency document associated this article can be found, in online version.

Declaration of competing interest

We declare no competing interests.

Acknowledgements

We thank Stefan Scheidelaar, Barend Elenbaas, and Kees van Walree for helpful discussions. We are grateful to Bonny W. M. Kuipers for support in DLS analysis, as well as Polyscope Polymers for providing the SMAnh (Xiran 30010) copolymer.

Financial support received from the European Union via the seventh framework program (Marie Curie Initial Training Network “ManiFold,” grant 317371 to J.M.D.) is gratefully acknowledged. This work was further supported financially by the Division of Chemical Sciences (CW) of the Netherlands Organisation for Scientific Research (NWO), via ECHO grant No. 711-017-006 (A.H.K). Finally we would like to acknowledge further financial support from the Erasmus+, EU exchange

program and traineeship, 2018/19, University of Turin, call No. 1320 (F.A.).

References

[1] C. Sun, S. Benlekbir, P. Venkatakrishnan, Y. Wang, S. Hong, J. Hosler, E. Tajkhorshid, J.L. Rubinstein, R.B. Gennis, Structure of the alternative complex III in a supercomplex with cytochrome oxidase, Nat. Lett. 557 (2018) 123–126, https://doi.org/10.1038/s41586-018-0061-y.

[2] M. Damian, V. Pons, P. Renault, C.M. Kadmi, B. Delort, L. Hartmann, GHSR-D2R heteromerization modulates dopamine signaling through an effect on G protein conformation, Proc. Natl. Acad. Sci. 115 (2018) 4501–4506, https://doi.org/10.1073/pnas.1712725115.

[3] J.M. Dörr, M.C. Koorengevel, M. Schäfer, A.V. Prokofyev, S. Scheidelaar, E.A.W. van der Cruijsen, T.R. Dafforn, M. Baldus, J.A. Killian, Detergent-free isolation, characterization, and functional reconstitution of a tetrameric K+ channel: the power of native nanodiscs, Proc. Natl. Acad. Sci. 111 (2014) 18607–18612, https://doi.org/10.1073/pnas.1416205112.

[4] E. Calzada, E. Avery, P.N. Sam, A. Modak, C. Wang, J.M. Mccaffery, X. Han, N.N. Alder, S.M. Claypool, Phosphatidylethanolamine made in the inner mitochondrial membrane is essential for yeast cytochrome bc1 complex function, Nat. Commun. 10 (2019), https://doi.org/10.1038/s41467-019-09425-1.

[5] A.R. Long, C.C.O. Brien, K. Malhotra, C.T. Schwall, A.D. Albert, A. Watts, N.N. Alder, A detergent-free strategy for the reconstitution of active enzyme complexes from native biological membranes into nanoscale discs, BMC Biotechnol. 13 (2013) 1–11 https://bmcbiotechnol.biomedcentral.com/articles/10.1186/1472-6750-13-41.

[6] D.J.K. Swainsbury, S. Scheidelaar, R. Van Grondelle, J.A. Killian, M.R. Jones, Bacterial reaction centers purified with styrene maleic acid copolymer retain native membrane functional properties and display enhanced stability, Angew. Chem. Int. Ed. 53 (2014) 11803–11807, https://doi.org/10.1002/anie.201406412.

[7] S. Gulati, M. Jamshad, T.J. Knowles, K.A. Morrison, R. Downing, N. Cant, R. Collins, J.B. Koenderink, R.C. Ford, M. Overduin, I.D. Kerr, T.R. Dafforn, A.J. Rothnie, Detergent-free purification of ABC (ATP-binding-cassette) transporters, Biochem. J. 461 (2014) 269–278, https://doi.org/10.1042/BJ20131477.

[8] T. Laursen, J. Borch, C. Knudsen, K. Bavishi, F. Torta, H.J. Martens, D. Silvestro, N.S. Hatzakis, M.R. Wenk, T.R. Dafforn, C.E. Olsen, M.S. Motawia, B. Hamberger, B.L. Møller, J.-E. Bassard, Characterization of a dynamic metabolon producing the defense compound dhurrin in sorghum, Science. 354 (2016) 890–893, https://doi.org/10.1126/science.aag2347.

[9] M. Parmar, S. Rawson, C.A. Scarff, A. Goldman, T.R. Dafforn, S.P. Muench, V.L.G. Postis, Using a SMALP platform to determine a sub-nm single particle cryo-EM membrane protein structure, Biochim. Biophys. Acta Biomembr. 1860 (2018) 378–383, https://doi.org/10.1016/j.bbamem.2017.10.005.

[10] M. Barniol-Xicota, S.H.L. Verhelst, Stable and functional rhomboid proteases in lipid nanodiscs by using diisobutylene/maleic acid copolymers, J. Am. Chem. Soc. 140 (2018) 14557–14561, https://doi.org/10.1021/jacs.8b08441.

[11] I. Prabudiansyah, I. Kusters, A. Caforio, A.J.M. Driessen, Characterization of the annular lipid shell of the Sec translocon, Biochim. Biophys. Acta Biomembr. 1848 (2015) 2050–2056, https://doi.org/10.1016/j.bbamem.2015.06.024.

[12] Y. Liu, E.C.C.M. Moura, J.M. Dörr, S. Scheidelaar, M. Heger, M.R. Egmond, J.A. Killian, T. Mohammadi, E. Breukink, Bacillus subtilis MraY in detergent-free system of nanodiscs wrapped by styrene-maleic acid copolymers, PLoS One 13 (2018) 1–18, https://doi.org/10.1371/journal.pone.0206692.

[13] J. Radoicic, S.H. Park, S.J. Opella, Macrodiscs comprising SMALPs for oriented sample solid-state NMR spectroscopy of membrane proteins, Biophys. J. 115 (2018) 22–25, https://doi.org/10.1016/j.bpj.2018.05.024.

[14] E. Reading, Z. Hall, C. Martens, T. Haghighi, H. Findlay, Z. Ahdash, A. Politis, P.J. Booth, Interrogating membrane protein conformational dynamics within native lipid compositions, Angew. Chem. Int. Ed. 56 (2017) 15654–15657, https://doi.org/10.1002/anie.201709657.

[15] S. Scheidelaar, M.C. Koorengevel, J.J. Dominguez Pardo, J.D. Meeldijk, E. Breukink, J.A. Killian, Molecular model for the solubilization of membranes into nanodisks by styrene maleic acid copolymers, Biophys. J. 108 (2015) 279–290, https://doi.org/10.1016/j.bpj.2014.11.3464.

[16] J.J. Dominguez Pardo, J.M. Dörr, A. Iyer, R.C. Cox, S. Scheidelaar, M.C. Koorengevel, V. Subramaniam, J.A. Killian, Solubilization of lipids and lipid phases by the styrene–maleic acid copolymer, Eur. Biophys. J. 46 (2017) 91–101, https://doi.org/10.1007/s00249-016-1181-7.

[17] R.C. Arenas, B. Danielczak, A. Martel, L. Porcar, C. Breyton, C. Ebel, S. Keller, Fast collisional lipid transfer among polymer-bounded nanodiscs, Sci. Rep. 7 (2017) 1–8, https://doi.org/10.1038/srep45875.

[18] S.C. Lee, T.J. Knowles, V.L.G. Postis, M. Jamshad, R.A. Parslow, Y.P. Lin, A. Goldman, P. Sridhar, M. Overduin, S.P. Muench, T.R. Dafforn, A method for detergent-free isolation of membrane proteins in their local lipid environment, Nat. Protoc. 11 (2016) 1149–1162, https://doi.org/10.1038/nprot.2016.070.

[19] B. Danielczak, A. Meister, S. Keller, Influence of Mg^{2+} and Ca^{2+} on nanodisc formation by diisobutylene/maleic acid (DIBMA) copolymer, Chem. Phys. Lipids 221 (2019) 30–38, https://doi.org/10.1016/j.chemphyslip.2019.03.004.

[20] M.C. Fiori, Y. Jiang, G.A. Altenberg, H. Liang, Polymer-encased nanodiscs with improved buffer compatibility, Sci. Rep. 7 (2017) 1–10, https://doi.org/10.1038/s41598-017-07110-1.

[21] S. Scheidelaar, M.C. Koorengevel, C.A. Van Walree, J.J. Dominguez, J.M. Dörr, J.A. Killian, Effect of polymer composition and ph on membrane solubilization by styrene-maleic acid copolymers, Biophys. J. 111 (2016) 1974–1986, https://doi.org/10.1016/j.bpj.2016.09.025.

[22] S.C.L. Hall, C. Tognoloni, J. Charlton, É.C. Bragginton, A.J. Rothnie, P. Sridhar, M. Wheatley, T.J. Knowles, T. Arnold, K.J. Edler, T.R. Dafforn, An acid-compatible co-polymer for the solubilization of membranes and proteins into lipid bilayer-containing nanoparticles, Nanoscale. 10 (2018) 10609–10619, https://doi.org/10.1039/c8nr01322e.

[23] T. Ravula, N.Z. Hardin, S.K. Ramadugu, A. Ramamoorthy, pH tunable and divalent metal ion tolerant polymer lipid nanodiscs, Langmuir. 33 (2017) 10655–10662, https://doi.org/10.1021/acs.langmuir.7b02887.

[24] R. Cuevas Arenas, J. Klingler, C. Vargas, S. Keller, Influence of lipid bilayer properties on nanodisc formation mediated by styrene/maleic acid copolymers, Nanoscale. 8 (2016) 15016–15026, https://doi.org/10.1039/c6nr02089e.

[25] J.J. Dominguez Pardo, J.M. Dörr, M.F. Renne, T. Ould-braham, M.C. Koorengevel, M.J. van Steenbergen, J.A. Killian, Thermotropic properties of phosphatidylcholine nanodiscs bounded by styrene-maleic acid copolymers, Chem. Phys. Lipids 208 (2017) 58–64, https://doi.org/10.1016/j.chemphyslip.2017.08.010.

[26] O. Korotych, J. Mondal, K.M. Gattás-Asfura, J. Hendricks, B.D. Bruce, Evaluation of commercially available styrene-co-maleic acid polymers for the extraction of membrane proteins from spinach chloroplast thylakoids, Eur. Polym. J. 114 (2019) 485–500, https://doi.org/10.1016/j.eurpolymj.2018.10.035.

[27] K.A. Morrison, A. Akram, A. Mathews, Z.A. Khan, J.H. Patel, C. Zhou, D.J. Hardy, C. Moore-Kelly, R. Patel, V. Odiba, T.J. Knowles, M.-u.-H. Javed, N.P. Chmel, T.R. Dafforn, A.J. Rothnie, Membrane protein extraction and purification using styrene-maleic acid (SMA) copolymer: effect of variations in polymer structure, Biochem. J. 473 (2016) 4349–4360, https://doi.org/10.1042/BCJ20160723.

[28] D.J.K. Swainsbury, S. Scheidelaar, N. Foster, R. Van Grondelle, J.A. Killian, M.R. Jones, The effectiveness of styrene-maleic acid (SMA) copolymers for solubilisation of integral membrane proteins from SMA-accessible and SMA-resistant membranes, BBA - Biomembr. 1859 (2017) 2133–2143, https://doi.org/10.1016/j.bbamem.2017.07.011.

[29] K. Skaar, H.J. Korza, M. Tarry, P. Sekyrova, M. Högbom, Expression and subcellular distribution of GFP-tagged human tetraspanin proteins in Saccharomyces cerevisiae, PLoS One 10 (2015) 1–19, https://doi.org/10.1371/journal.pone.0134041.

[30] A. Grethen, A.O. Oluwole, B. Danielczak, C. Vargas, S. Keller, Thermodynamics of nanodisc formation mediated by styrene/maleic acid (2:1) copolymer, Sci. Rep. 7 (2017) 1–14, https://doi.org/10.1038/s41598-017-11616-z.

[31] J.J. Dominguez Pardo, M.C. Koorengevel, N. Uwugiaren, J. Weijers, A.H. Kopf, J.J. Domı, H. Jahn, C.A. Van Walree, M.J. Van Steenbergen, J.A. Killian, Membrane solubilization by styrene-maleic acid copolymers: delineating the role of polymer length, Biophys. J. 115 (2018) 129–138, https://doi.org/10.1016/j.bpj.2018.05.032.

[32] H. Schrempf, O. Schmidt, R. Kümmerlen, S. Hinnah, D. Müller, M. Betzler, T. Steinkamp, R. Wagner, A prokaryotic potassium ion channel with two predicted transmembrane segments from Streptomyces lividans, EMBO J. 14 (1995) 5170–5178, https://doi.org/10.1002/j.1460-2075.1995.tb00201.x.

[33] A. Van Dalen, H. Schrempf, J.A. Killian, B. De Kruijff, Efficient membrane assembly of the KcsA potassium channel in Escherichia coli requires the protonmotive force, EMBO Rep. 1 (2000) 340–346.

[34] D.M. Cortes, E. Perozo, Structural dynamics of the Streptomyces lividans K+ channel (SKC1): oligomeric stoichiometry and stability, Biochemistry. 36 (1997) 10343–10352, https://doi.org/10.1021/bi971018y.

[35] A.H. Kopf, M.C. Koorengevel, C.A. Van Walree, T.R. Dafforn, J.A. Killian, A simple and convenient method for the hydrolysis of styrene-maleic anhydride copolymers to styrene-maleic acid copolymers, Chem. Phys. Lipids 218 (2019) 85–90, https://doi.org/10.1016/j.chemphyslip.2018.11.011.

[36] E.G. Bligh, W.J. Dyer, A rapid method of total lipid extraction and purification, Can. J. Biochem. Physiol. 37 (1959) 911–917, https://doi.org/10.1139/o59-099.

[37] G. Rouser, S. Fleischer, A. Yamamoto, Two dimensional thin layer chromatographic separation of polar lipids and determination of phospholipids by phosphorus analysis of spots, Lipids. 5 (1970) 494–495.

[38] G. Daum, P.C. Bohni, G. Schatzg, Import of proteins into mitochondria, J. Biol. Chem. 257 (1982) 13028–13033.

[39] J.M. Dörr, S. Scheidelaar, M.C. Koorengevel, J.J. Dominguez, M. Schäfer, C.A. van Walree, J.A. Killian, The styrene–maleic acid copolymer: a versatile tool in membrane research, Eur. Biophys. J. 45 (2016) 3–21, https://doi.org/10.1007/s00249-015-1093-y.

[40] S. Morein, A.S. Andersson, L. Rilfors, G. Lindblom, Wild-type Escherichia coli cells regulate the membrane lipid composition in a "window" between gel and non-lamellar structures, J. Biol. Chem. 271 (1996) 6801–6809, https://doi.org/10.1074/jbc.271.12.6801.

[41] S.E. Horvath, G. Daum, Lipids of mitochondria, Prog. Lipid Res. 52 (2013) 590–614, https://doi.org/10.1016/j.plipres.2013.07.002.

[42] C. Vargas, R.C. Arenas, E. Frotscher, S. Keller, Nanoparticle self-assembly in mixtures of phospholipids with styrene/maleic acid copolymers or fluorinated surfactants, Nanoscale. 7 (2015) 20685–20696, https://doi.org/10.1039/c5nr06353a.

[43] A.C.K. Teo, S.C. Lee, N.L. Pollock, Z. Stroud, S. Hall, A. Thakker, A.R. Pitt, T.R. Dafforn, C.M. Spickett, D.I. Roper, Analysis of SMALP co-extracted phospholipids shows distinct membrane environments for three classes of bacterial membrane protein, Sci. Rep. 9 (2019) 1–10, https://doi.org/10.1038/s41598-018-37962-0.

[44] M.G. Karlova, N. Voskoboynikova, G.S. Gluhov, D. Abramochkin, O.A. Malak, A. Mulkidzhanyan, G. Loussouarn, H.J. Steinhoff, K.V. Shaitan, O.S. Sokolova, Detergent-free solubilization of human Kv channels expressed in mammalian cells, Chem. Phys. Lipids 219 (2019) 50–57, https://doi.org/10.1016/j.chemphyslip.2019.01.013.

[45] T.J. Silhavy, D. Kahne, S. Walker, The bacterial cell envelope, Cold Spring Harb. Perspect. Biol. 2 (2010) 1–16, https://doi.org/10.1101/cshperspect.a000414.
[46] A.J. Bell, L.K. Frankel, T.M. Bricker, High yield non-detergent isolation of photosystem I-light-harvesting chlorophyll II membranes from spinach thylakoids, J. Biol. Chem. 290 (2015) 18429–18437, https://doi.org/10.1074/jbc.m115.663872.
[47] K. Kato, Y. Bito, Gel to liquid-crystalline phase transitions of lipids and membranes isolated from Escherichia coli cells, Microbiol. Immunol. 24 (1980) 703–716.
[48] W. Dowhan, Molecular basis for membrane phospholipid diversity: why are there so many lipids? Annu. Rev. Biochem. 66 (1997) 199–232, https://doi.org/10.1146/annurev.biochem.66.1.199.
[49] K. Yasuhara, J. Arakida, T. Ravula, S.K. Ramadugu, B. Sahoo, J. Kikuchi, A. Ramamoorthy, Spontaneous lipid nanodisc fomation by amphiphilic polymethacrylate copolymers, J. Am. Chem. Soc. 139 (2017) 18657–18663, https://doi.org/10.1021/jacs.7b10591.
[50] N.Z. Hardin, T. Ravula, G. Di Mauro, A. Ramamoorthy, Hydrophobic functionalization of polyacrylic acid as a versatile platform for the development of polymer lipid nanodisks, Small. 15 (2019) 1–5, https://doi.org/10.1002/smll.201804813.
[51] T. Ravula, N.Z. Hardin, S.K. Ramadugu, S.J. Cox, A. Ramamoorthy, N.Z. Hardin, S.K. Ramadugu, S.J. Cox, A. Ramamoorthy, pH resistant monodispersed polymer-lipid nanodiscs, Angew. Chem. Int. Ed. 57 (2018) 1342–1345, https://doi.org/10.1002/anie.201712017.pH.
[52] R. Schwartz, C.S. Ting, J. King, Whole proteome pl values correlate with subcellular localizations of proteins for organisms within the three domains of life, Genome Res. 11 (2001) 703–709, https://doi.org/10.1101/gr.GR-1587R.
[53] R.A. Van Bogelen, E.E. Schiller, J.D. Thomas, F.C. Neidhardt, Diagnosis of cellular states of microbial organisms using proteomics, Electrophoresis. 20 (2007) 2149–2159, https://doi.org/10.1002/9783527613489.ch2.
[54] A.J. Link, K. Robison, G.M. Church, Comparing the predicted and observed properties of proteins encoded in the genome of Escherichia coli K-12, Electrophoresis. 18 (1997) 1259–1313.
[55] T. Sato, K. Ito, T. Yura, Membrane proteins of Escherichia coli K-12: two-dimensional polyacrylamide gel electrophoresis of inner and outer membranes, Eur. J. Biochem. 78 (1977) 557–567, https://doi.org/10.1111/j.1432-1033.1977.tb11769.x.
[56] M. Pérez-Rodríguez, G. Prieto, C. Rega, L.M. Varela, F. Sarmiento, V. Mosquera, A comparative study of the determination of the critical micelle concentration by conductivity and dielectric constant measurements, Langmuir. 14 (1998) 4422–4426, https://doi.org/10.1021/la980296a.
[57] J.P. Marcolongo, M. Mirenda, Thermodynamics of sodium dodecyl sulfate (SDS) micellization: an undergraduate laboratory experiment, J. Chem. Educ. 88 (2011) 629–633, https://doi.org/10.1021/acs.jchemed.5b00934.